

ChemCatChem

Supporting Information

Pivotal Contribute of EPR-Characterized Persistent Free Radicals in the Methylene Blue Removal by a Bamboo-Based Biochar-Packed Column Flow System

Filippo Zanardi, Federica Romei, Mario Nogueira Barbosa Junior, Sidnei Paciornik, Paola Franchi, Marco Lucarini, Anna Turchetti, Lorenzo Poletti, Silvana Alfei,* and Omar Ginoble Pandoli*

Supplementary Materials

Pivotal Contribute of EPR-Characterized Persistent Free Radicals (PFRs) in the Methylene Blue Removal by a Bamboo-Based Biochar-Packed Column Flow System

Filippo Zanardi,^a Federica Romei,^a Mario Nogueira Barbosa Junior,^b Sidnei Paciornik,^b Paola Franchi,^c Marco Lucarini,^c Anna Turchetti,^c Lorenzo Poletti,^d Silvana Alfei,^{e,*} and Omar Ginoble Pandoli^{e,f,*}

^a Department of Chemistry and Industrial Chemistry, University of Genoa, Via Dodecaneso, 31, 16148, Genoa, Italy. zanardifilippo.01@gmail.com; federica.romei17@gmail.com

^b Departamento de Engenharia Química e de Materiais, Pontifícia Universidade Católica, Rua Marque de São Vicente, 225, 22451-900, Rio de Janeiro, Brazil. sidnei@puc-rio.br

^c Department of Chemistry "Giacomo Ciamician" Via P. Gobetti 85, 40129, Bologna, Italy. paola.franchi@unibo.it; marco.lucarini@unibo.it; anna.turchetti3@unibo.it

^d Department of Chemical, Pharmaceutical and Agricultural Sciences, Via L. Borsari, 46, 44121 Ferrara, Italy Lorenzo.poletti@unife.it

^e Department of Pharmacy, University of Genoa, Viale Cembrano, 4, 16148 Genoa, Italy

^f Departamento de Química, Pontifícia Universidade Católica, Rua Marquês de São Vicente, 225, 22451-900, Rio de Janeiro, Brazil.

*Correspondence: omar.ginoblepandoli@unige.it, omarpandoli@puc-rio.br; alfei@difar.unige.it

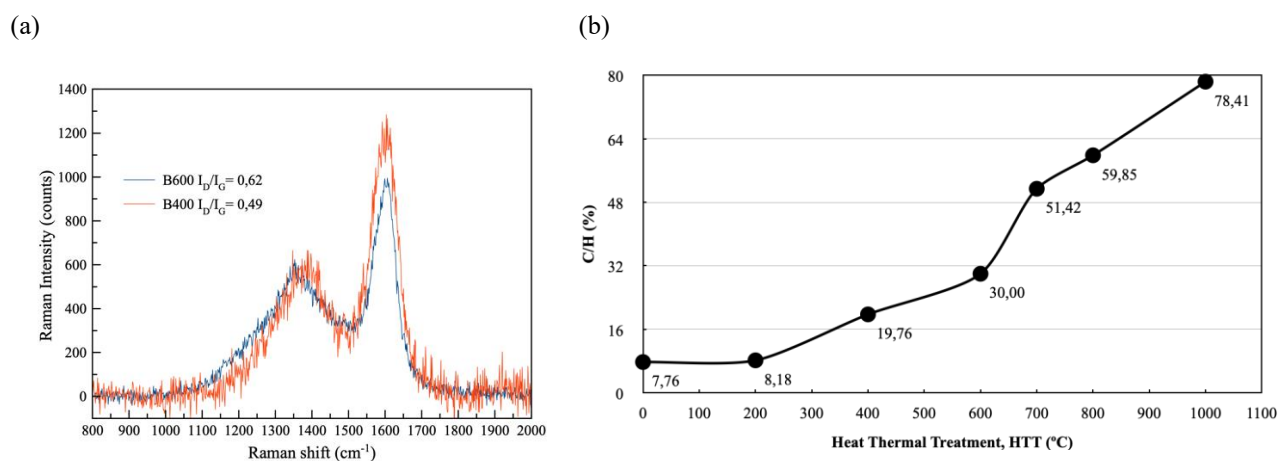


Fig. S1 (a) Raman spectra of B400 and B600; (b) elemental analysis of the pyrolysed bamboo samples at different temperatures.

Section S1: Kinetic Models

In this Section, we provided an as detailed as possible description of the kinetic models used by us in this study to investigate the main mechanisms governing the removal of methylene blue dye (MB) from MB solution by means a bamboo-derived biochar (B400).

Zero-Order Kinetic Model

The zero-order kinetic model (see its descriptive equation and values to be reported on x/y axis to have the related dispersion graph, in Table 3, in the main text) in absorption, describes a situation where the rate of absorption is constant and does not change with time or concentration. When the zero-order kinetic model well fits absorption over time experimental data, it means that a fixed quantity of substance is absorbed per unit of time, regardless of the concentration of the substance that remains to be absorbed[1–3]. Zero-order kinetics can occur under certain conditions, such as with a controlled-release of a substance in solution or when the absorption sites on the absorbent are saturated[1,2].

First-Order Kinetic Model

In the first-order kinetics (see its descriptive equation and values to be reported on x/y axis to have the related dispersion graph, in Table 3, in the main text), the rate of absorption is instead proportional to the concentration of the substance to be absorbed, in our case the concentration of MB in solution. This suggest that, if first order kinetic model would well fit experimental data of absorption over time, the rate of absorption should decrease over time proportionally to the reduction of the substance concentration in solution[2].

Pseudo-Second Order Kinetic Model

Pseudo-second order (PSO) model (see its descriptive equation and values to be reported on x/y axis to have the related dispersion graph, in Table 3, in the main text) is capable to describe many adsorption systems[4] and in our case well fit the most part of experimental data acquired during the study of the removal of MB, from MB solutions using biochar B400. The PSO model was firstly applied to model the adsorption of lead onto peat[5]. By fitting PSO model to the experimental data of absorption over time, it is possible to predict the quantity of absorbed substances at equilibrium (q_e) and to calculate the adsorption rate constants (K1 and K2). An exact correspondence with experimental data, in addition to the R^2 values of the linear regression associated to the model, confirms that the absorption system is well described by the PSO model. A good fit of PSO model with experimental data could depend by a low initial concentration of the substance in removal (C_0), and generally describes the adsorption by adsorbent materials where active sites are abundant, such as modified hydro char with respect to unmodified one [5,6]. In fact, the adsorption of pollutants on modified absorbents, thus providing active sites mainly responsible of their removal, were best described by the PSO model [5,6]. Collectively, in removal processes that fit PSO kinetics, electron transfer reactions as occur in presence of PFR, electrostatic interactions, and hydrogen bond formation are the main mechanisms governing the process.

Higuchi Kinetic Model

Usually, the Higuchi model is used to describe the mechanism of drug release[7]. Anyway, in some cases in this study, when used to fit with our experimental data of MB removal from MB solutions, Higuchi model resulted suitable to describe our system. Collectively, the Higuchi model is a law (see its descriptive equation and values to be reported on x/y axis to have the related

dispersion graph, in Table 3, in the main text) expressing a linear dependence of the released/removed amount of a substance, proportional to the square root of time, i.e. $t^{0.5}$ [8]. Such a linear dependence of the released/removed amount on the square root of time is frequently obtained in literature [8]. Since 0.5 represents the diffusional or transport exponent “ n ” often present in the equations of mathematical kinetic models and that for $n = 0.5$ the main mechanism of the release/removal from various non-swellable systems is Fickian diffusional, Higuchi model best describe absorption/removal processes mainly governed by physical diffusional mechanisms [7].

Korsmeyer-Peppas Kinetic Model

The Korsmeyer Peppas model (see its descriptive equation and values to be reported on x/y axis to have the related dispersion graph, in Table 3, in the main text) best describes absorption/removal processes governed mainly by mechanisms which could be diffusional or more complex not chemical processes (Case II or Super Case II transport) depending on the value of the diffusional or transport exponent n_{KP} [9]. The value of the release exponent n in the Korsmeyer-Peppas model could approach a value of one ($n = 1$), which corresponds to a case II transport mechanism, when the absorption/desorption process is predominately controlled by adsorbent relaxation and/or erosion[10]. This so-called anomalous diffusion (non Fickian) was likely due to swelling and relaxation of the adsorbent in the dissolution media.

Hixson-Crowell Kinetic Model

Hixson-Crowell kinetic model (see its descriptive equation and values to be reported on x/y axis to have the related dispersion graph, in Table 3, in the main text) describes a system where the cube root of removal efficiency on time t is linearly related to that time. It implies physic diffusional mechanisms and adsorbent surface alteration over time[11]. The removal processes which are well described by Hixson Crowell kinetics, are typically characterised by adsorbent systems whose surface alters over time [11].

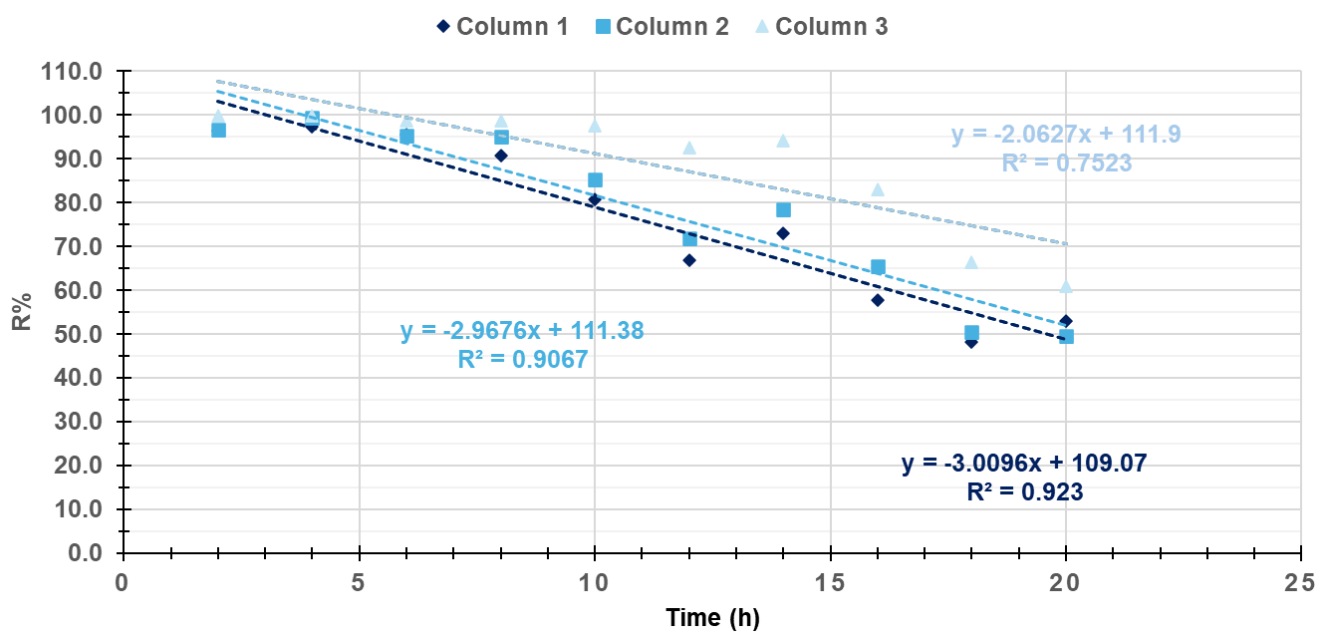


Fig. S2 Zero-order kinetic models.

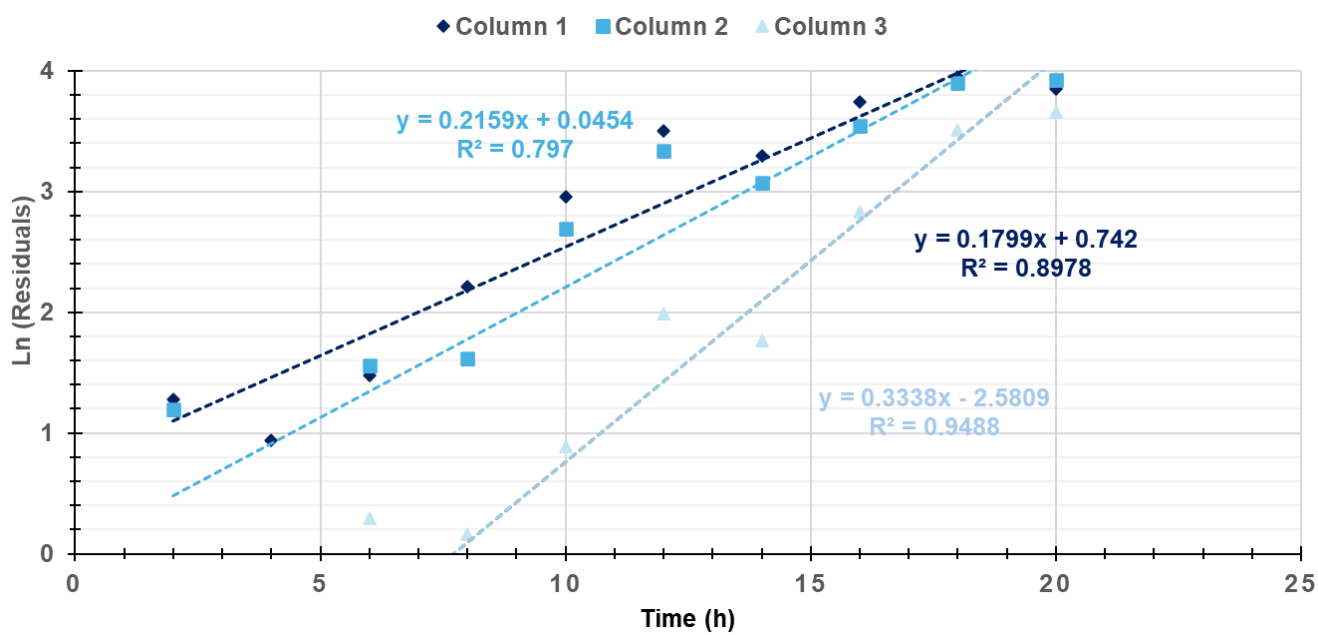


Fig. S3 First-order kinetic models.

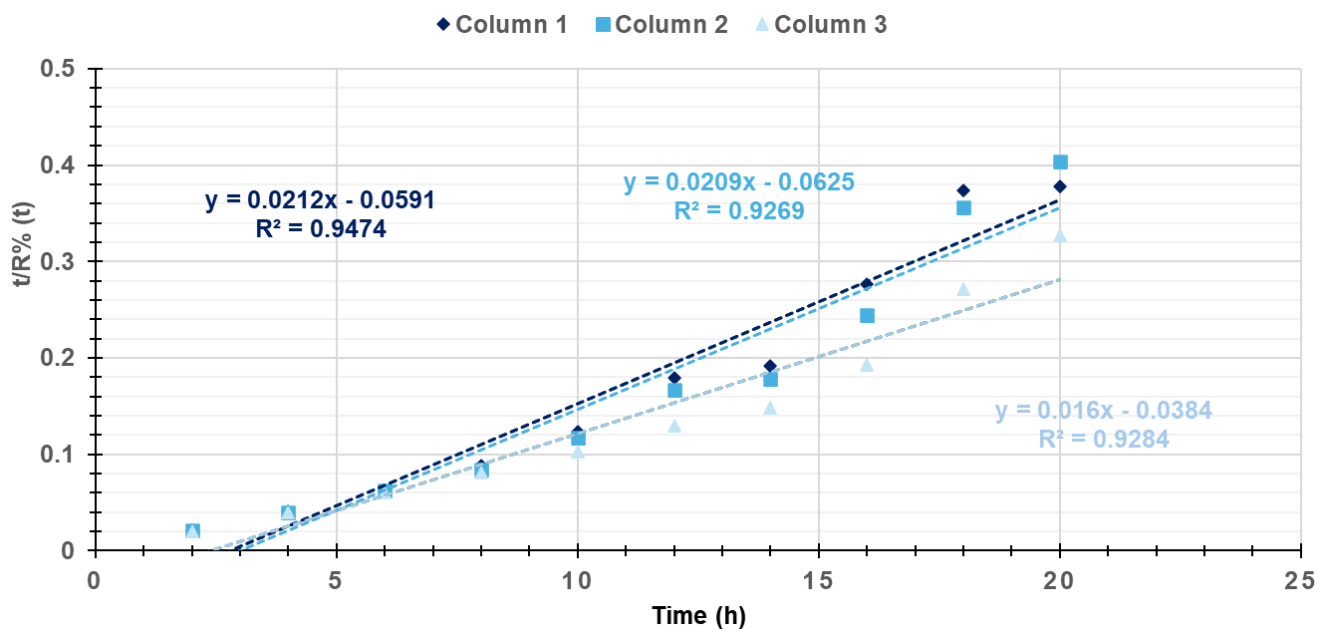


Fig. S4 Pseudo-second order (PSO) kinetic models.

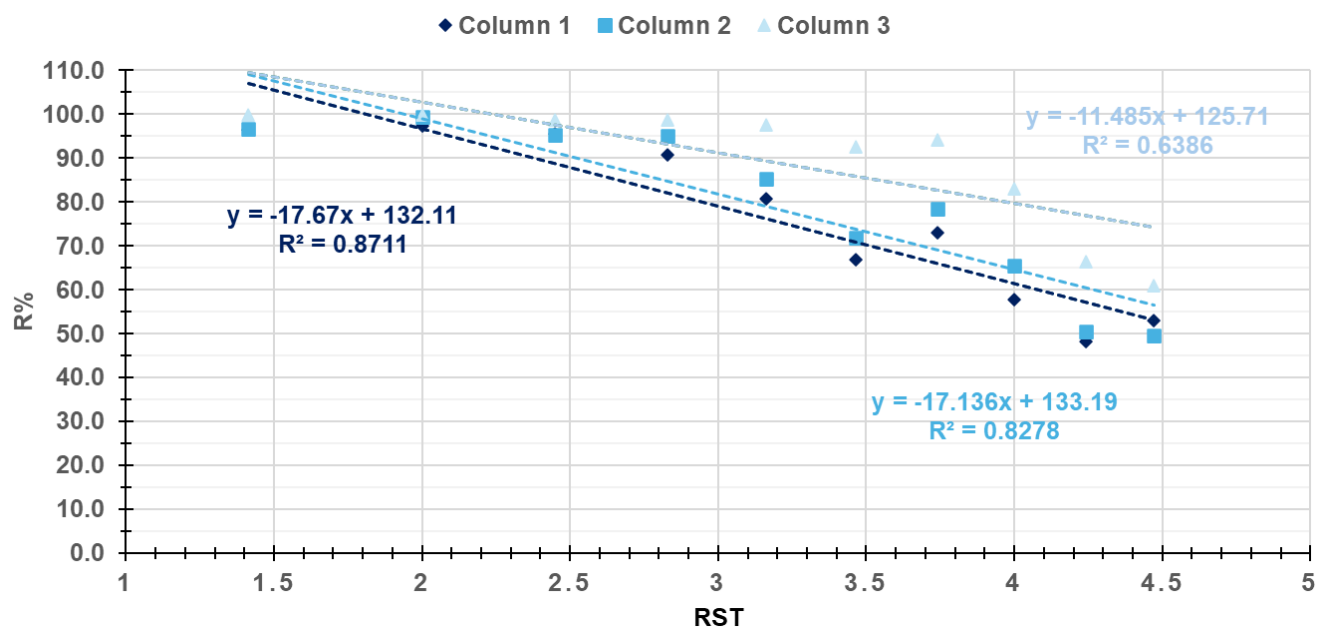


Fig. S5 Higuchi kinetic models. RST = root square of time.

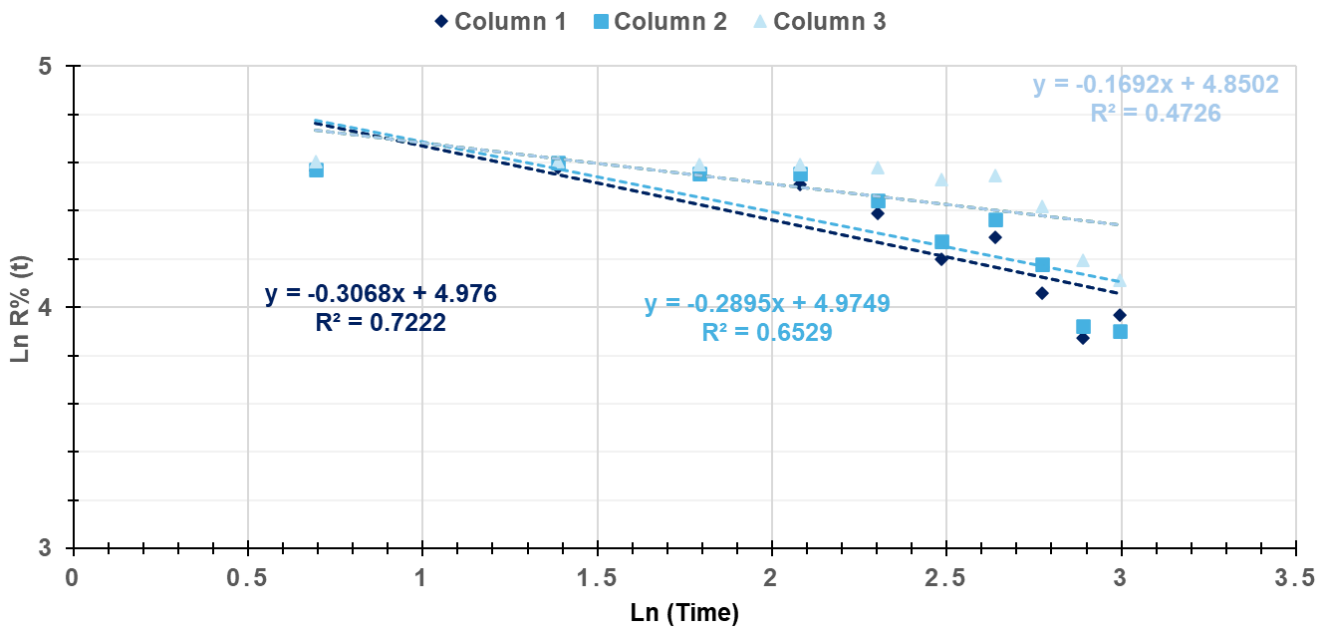


Fig. S6 Korsmeyer Peppas kinetic models.

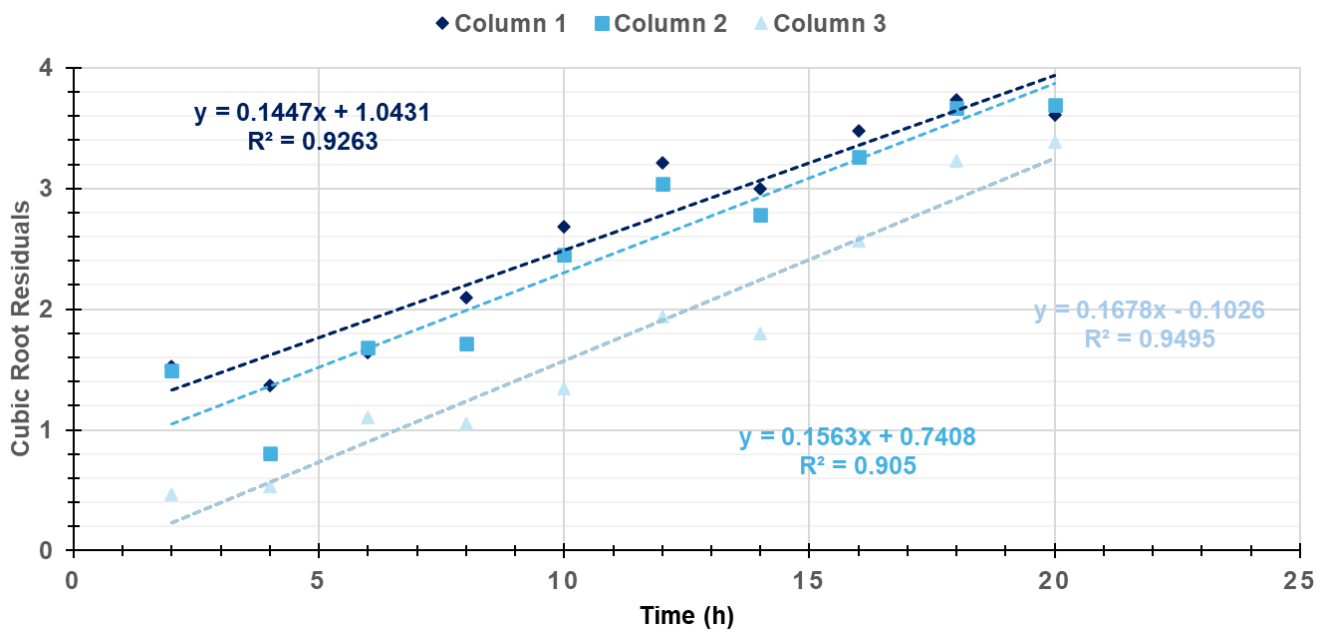


Fig. S7 Hixson Crowell kinetic models.

Table S1. R^2 values of all kinetic models considered for each column.

Models	R^2 Column 1	R^2 Column 2	R^2 Column 3
Zero-order	0.9230	0.9067	0.7523
First-order	0.8978	0.7970	0.9488
PSO *	0.9475	0.9269	0.9284
Higuchi	0.8711	0.8278	0.6386
Korsmeyer Peppas	0.7222	0.6529	0.4726
Hixson Crowell	0.9263	0.9050	0.9495

* Pseudo second-order model. In bold the highest R^2 values.

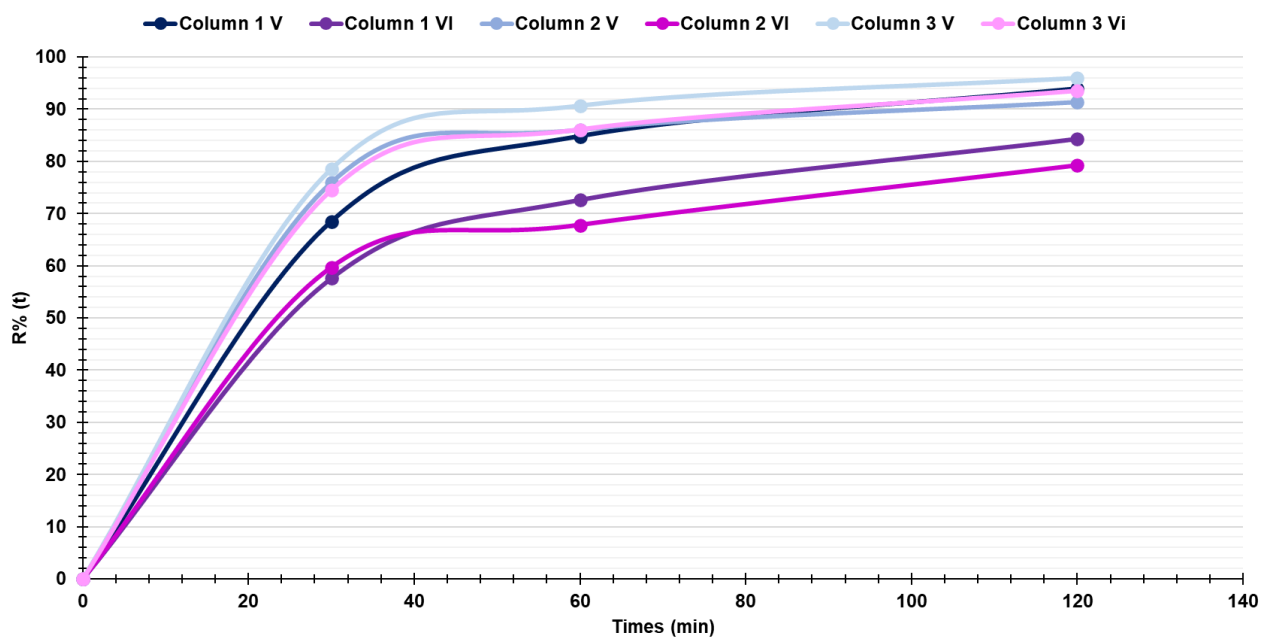


Fig. S8 Removal efficiency (R%) measured at 30, 60 and 120 minutes for columns 1, 2 and 3 within cycles 5 (dark blue, light blue, and very light blue lines) and 6 (purple, light purple, and pink lines).

Table S2. R^2 values of all kinetic model considered for each column.

Models	R^2 Col. 1 V	R^2 Col.1 VI	R^2 Col.2 V	R^2 Col.2 VI	R^2 Col.3 V	R^2 Col.3 VI
Zero-order	0.6911	0.7388	0.6042	0.6887	0.6128	0.6364
First-order	0.9488	0.9228	0.8255	0.8549	0.9026	0.8993
PSO *	0.9890	0.9814	0.9964	0.9875	0.9962	0.9945
Higuchi	0.9266	0.9517	0.8716	0.9233	0.8778	0.8931
Korsmeyer	0.9600	0.9848	0.9602	0.9967	0.9414	0.9756
Peppas						
Hixson Crowell	0.8688	0.8652	0.7420	0.7981	0.7974	0.8066

* Pseudo second-order model. In bold the highest R^2 values.

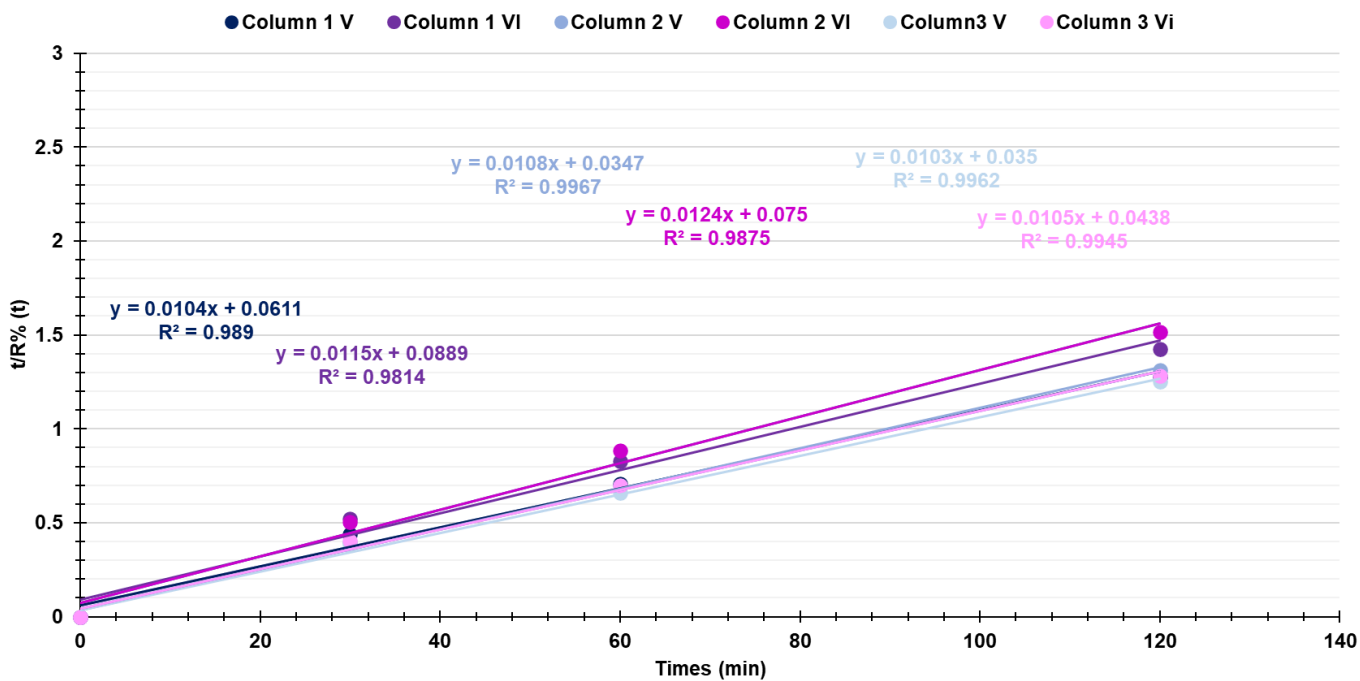


Fig. S9. PSO kinetic models.

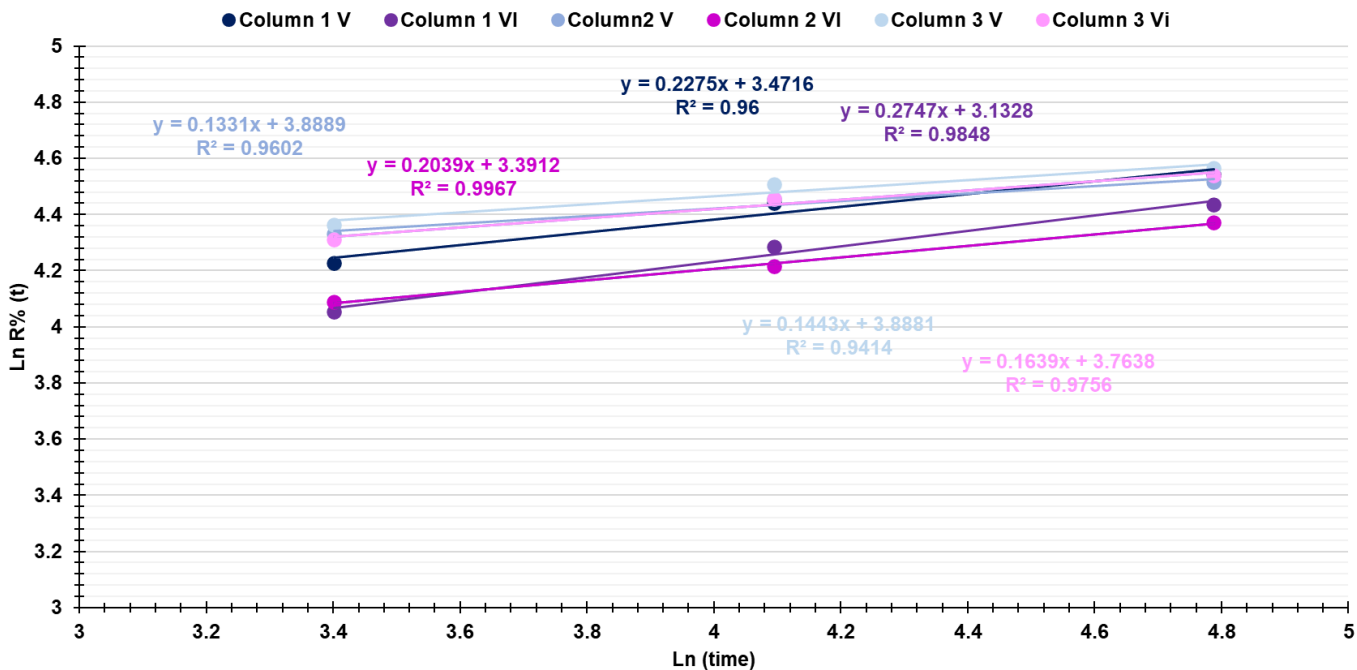


Fig. S10 Korsmeyer Peppas kinetic models.

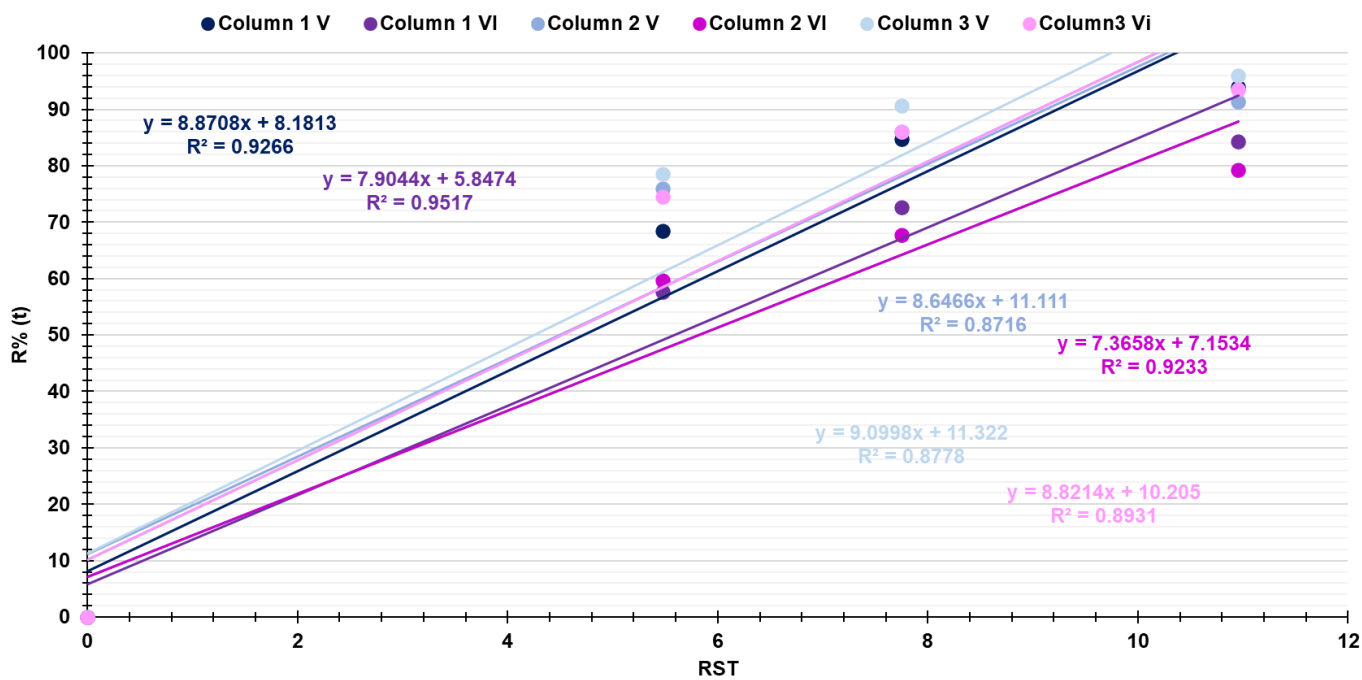


Fig. S11 Higuchi kinetic models.

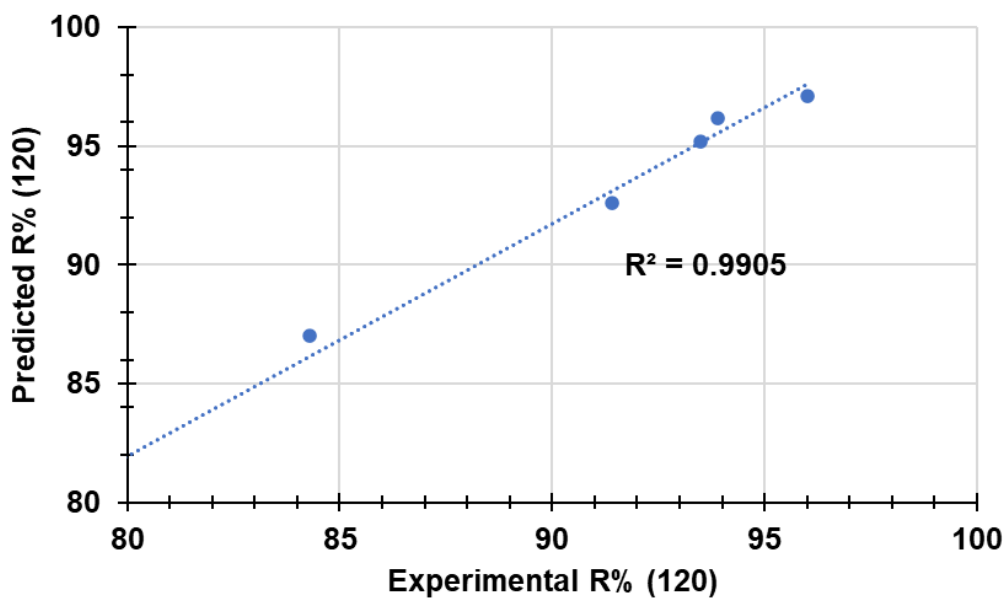


Fig. S12 Correlation between the experimental values of R% measured after 120 minutes treatment of a MB solution by columns 1, 2 and 3 in cycles 5 and 6 and those predicted by PSO model.

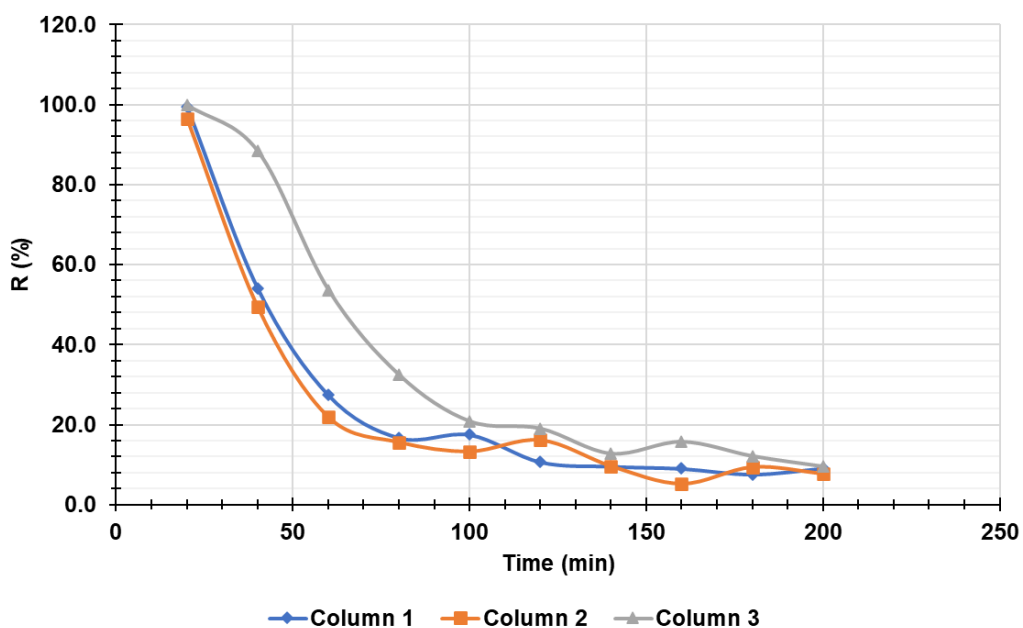


Fig. S13 MB removal percentage over time by column 1 (blue), column 2 (orange) and column 3 (grey).

Table S3. R^2 values of all kinetic model considered for each column.

Models	R^2 Column 1	R^2 Column 2	R^2 Column 3
Zero-order	0.6183	0.5843	0.7820
First-order	0.3615	0.3930	0.5410
PSO *	0.9527	0.8173	0.9092
Higuchi	0.7497	0.7152	0.8778
Korsmeyer Peppas	0.9712	0.9251	0.9336
Hixson Crowell	0.4463	0.4550	0.5958

* Pseudo second-order model. In bold the highest R^2 values.

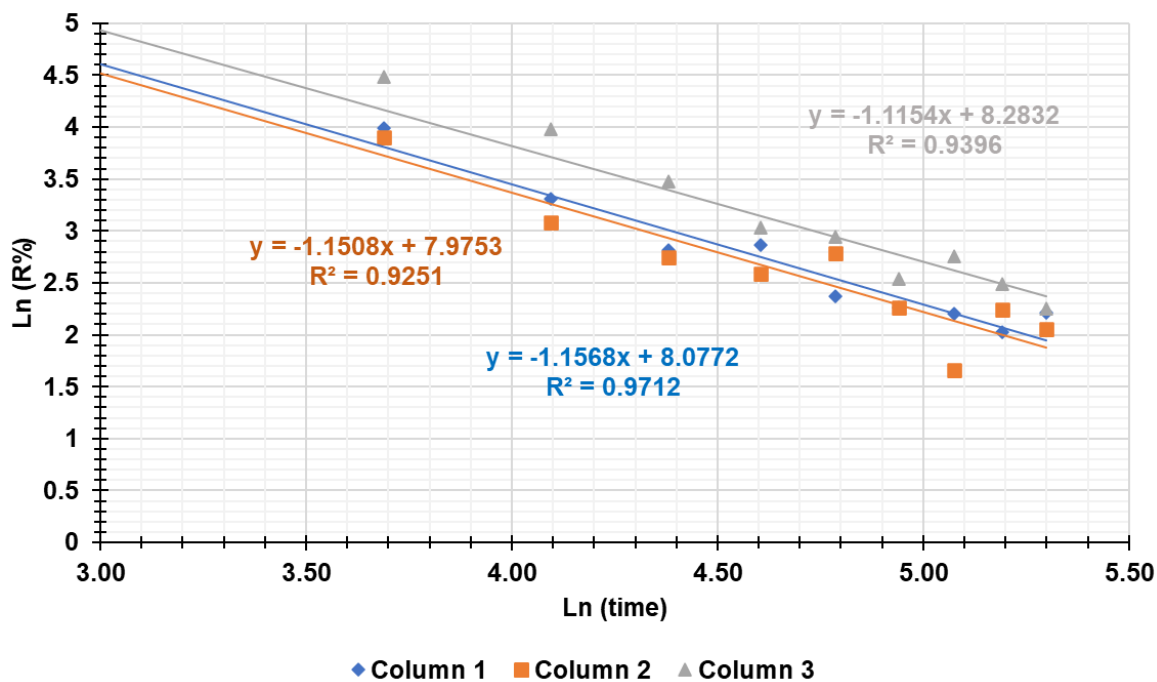


Fig. S14 Korsmeyer Peppas kinetic models.

Table S4. R² values of all kinetic model considered for each column.

Models	R ² Col. 1	R ² Col.2	R ² Col.3	R ² Col.4	R ² Col.5	R ² Col.6	R ² Col.7
Zero order	0.7578	0.6488	0.7211	0.9955	0.9882	0.9420	0.9984
First order	0.8196	0.4691	0.4354	0.8312	0.8598	0.9031	0.9711
PSO *	0.9855	0.9896	0.9991	0.8356	0.7875	0.7978	0.9406
Higuchi	0.7268	0.3911	0.3748	0.9053	0.9270	0.9528	0.9910
Korsmeyer Peppas	0.5395	0.4436	0.5743	0.8266	0.7776	0.7131	0.9382
Hixson Crowell	0.8118	0.5808	0.8432	0.9199	0.9441	0.9496	0.9837

* Pseudo second-order model. In bold the highest R² values.

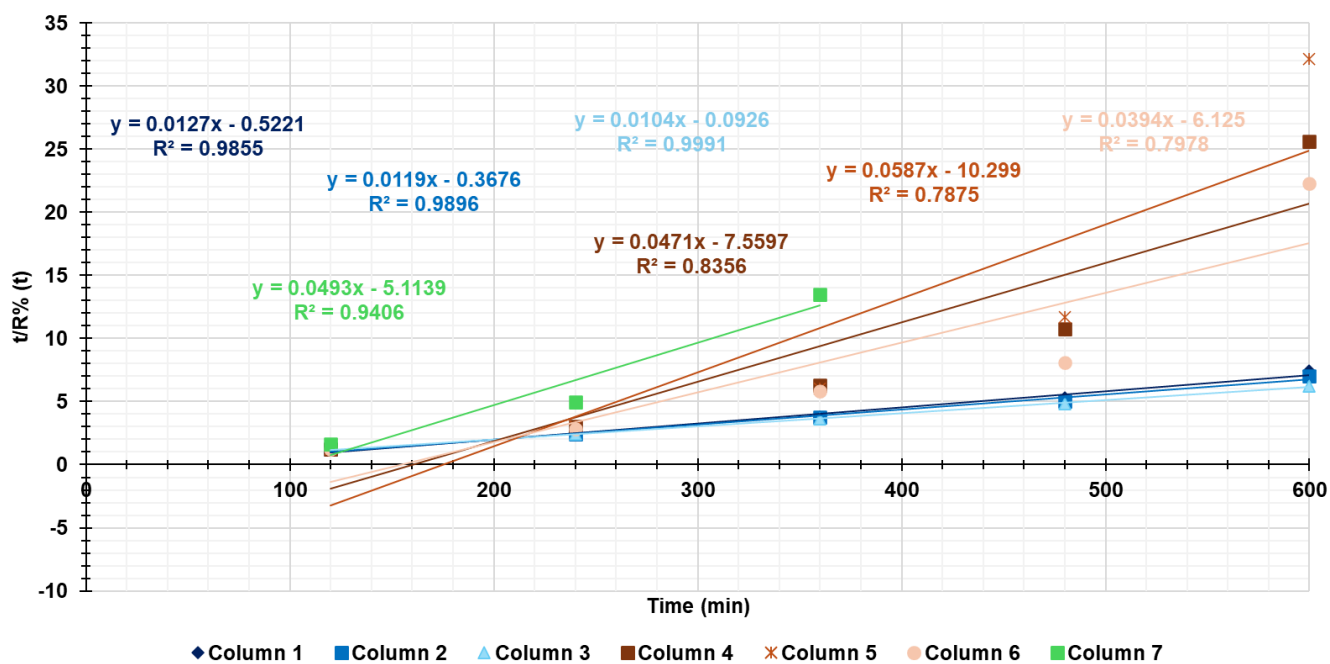


Fig. S15 PSO kinetic models.

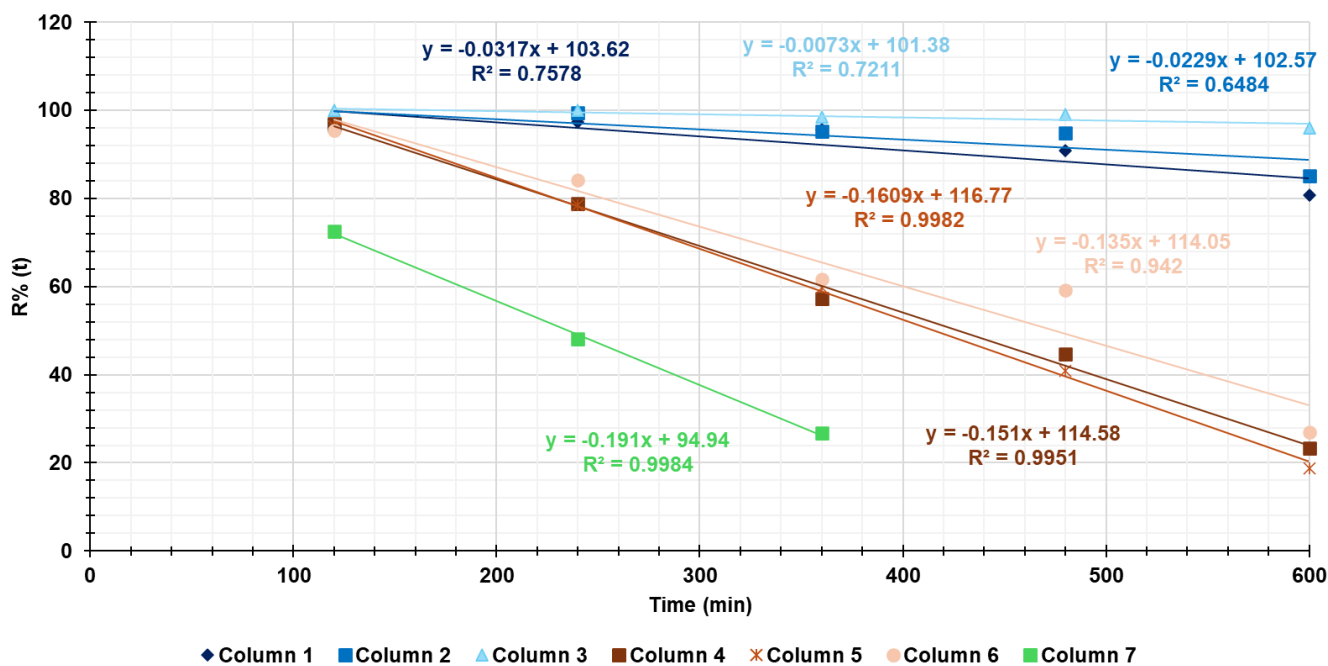


Fig. S16 Zero-order kinetic models.

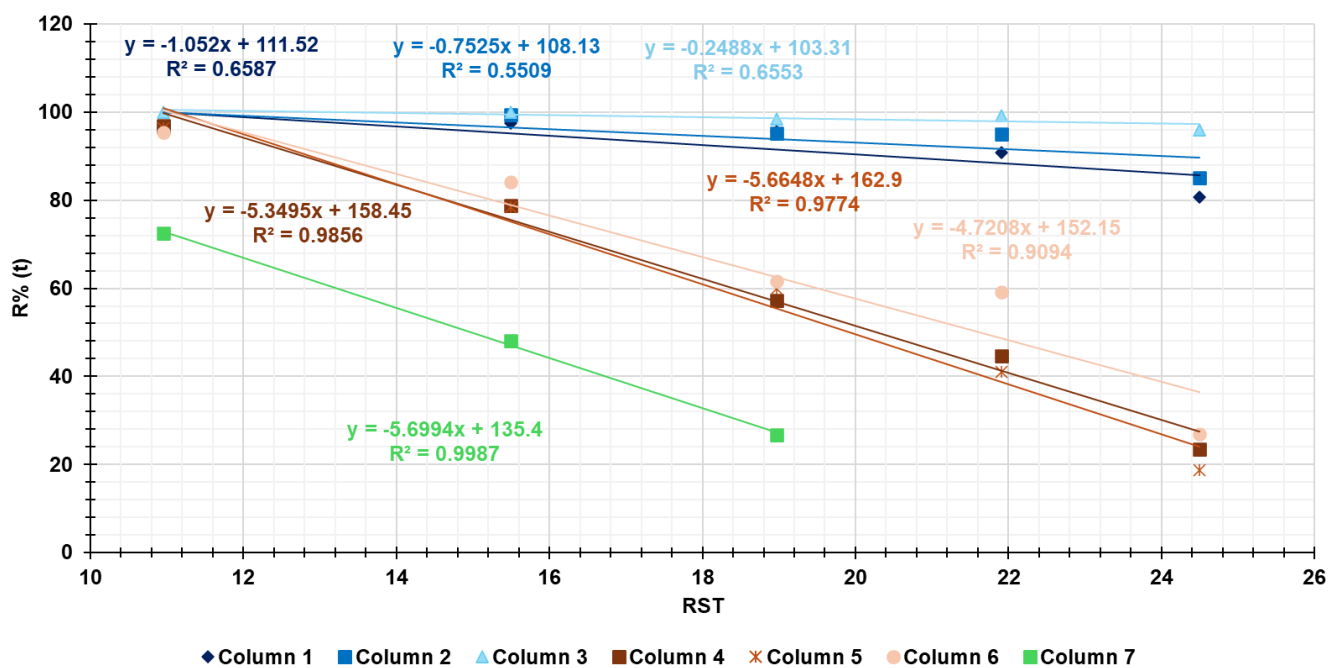


Fig. S17 Higuchi kinetic models. RST = root square of time.

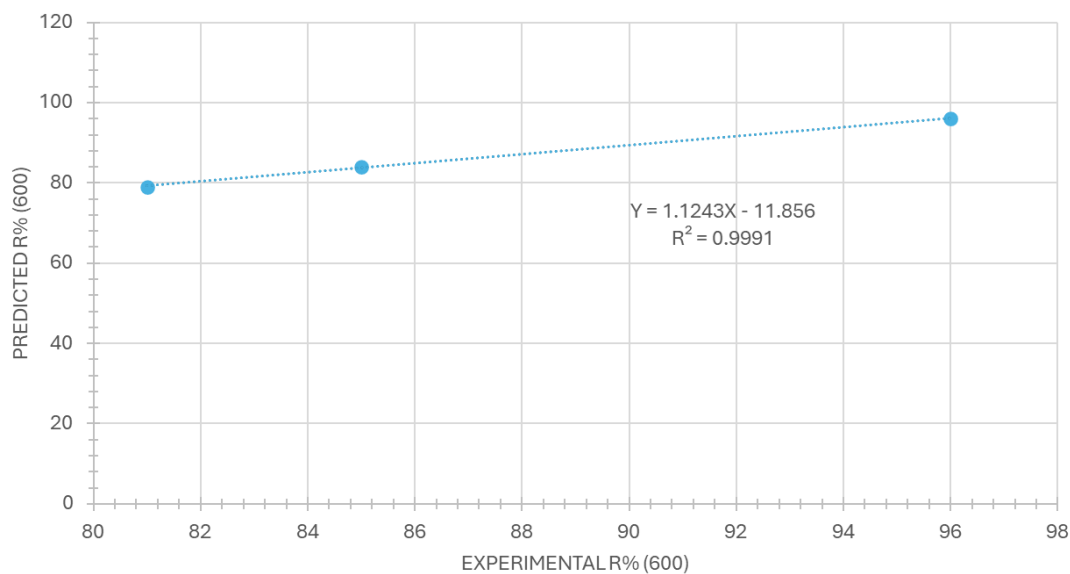


Fig. S18 Correlation between the experimental values of R% measured after 600 minutes treatment of a MB solution by columns 1, 2 and 3 and those predicted by PSO model.

References

1. Zou, H.; Banerjee, P.; Leung, S.S.Y.; Yan, X. Application of Pharmacokinetic-Pharmacodynamic Modeling in Drug Delivery: Development and Challenges. *Front Pharmacol* **2020**, *11*, doi:10.3389/fphar.2020.00997.
2. Pharmacology Mentor First-Order vs. Zero-Order Kinetics: What You Need to Know Available online: <https://pharmacologymentor.com/first-order-vs-zero-order-kinetics/> (accessed on 18 July 2024).
3. Tarek A. Ahmed *Pharmacokinetics of Drugs Following IV Bolus, IV Infusion, and Oral Administration.*; Tarek A. Ahmed, Ed.; 2015;
4. Revellame, E.D.; Fortela, D.L.; Sharp, W.; Hernandez, R.; Zappi, M.E. Adsorption Kinetic Modeling Using Pseudo-First Order and Pseudo-Second Order Rate Laws: A Review. *Clean Eng Technol* **2020**, *1*, 100032, doi:10.1016/j.clet.2020.100032.
5. Wang, J.; Guo, X. Adsorption Kinetic Models: Physical Meanings, Applications, and Solving Methods. *J Hazard Mater* **2020**, *390*, 122156, doi:10.1016/j.jhazmat.2020.122156.
6. Xia, Y.; Yang, T.; Zhu, N.; Li, D.; Chen, Z.; Lang, Q.; Liu, Z.; Jiao, W. Enhanced Adsorption of Pb(II) onto Modified Hydrochar: Modeling and Mechanism Analysis. *Bioresour Technol* **2019**, *288*, 121593, doi:10.1016/j.biortech.2019.121593.
7. Valenti, G.E.; Marengo, B.; Milanese, M.; Zuccari, G.; Brullo, C.; Domenicotti, C.; Alfei, S. Imidazo-Pyrazole-Loaded Palmitic Acid and Polystyrene-Based Nanoparticles: Synthesis, Characterization and Antiproliferative Activity on Chemo-Resistant Human Neuroblastoma Cells. *Int J Mol Sci* **2023**, *24*, 15027, doi:10.3390/ijms241915027.

8. Mircioiu, C.; Voicu, V.; Anuta, V.; Tudose, A.; Celia, C.; Paolino, D.; Fresta, M.; Sandulovici, R.; Mircioiu, I. Mathematical Modeling of Release Kinetics from Supramolecular Drug Delivery Systems. *Pharmaceutics* **2019**, *11*, 140, doi:10.3390/pharmaceutics11030140.
9. Wu, I.Y.; Bala, S.; Škalko-Basnet, N.; di Cagno, M.P. Interpreting Non-Linear Drug Diffusion Data: Utilizing Korsmeyer-Peppas Model to Study Drug Release from Liposomes. *European Journal of Pharmaceutical Sciences* **2019**, *138*, 105026, doi:10.1016/j.ejps.2019.105026.
10. Guerra-Ponce, W.L.; Gracia-Vásquez, S.L.; González-Barranco, P.; Camacho-Mora, I.A.; Gracia-Vásquez, Y.A.; Orozco-Beltrán, E.; Felton, L.A. In Vitro Evaluation of Sustained Released Matrix Tablets Containing Ibuprofen: A Model Poorly Water-Soluble Drug. *Brazilian Journal of Pharmaceutical Sciences* **2016**, *52*, 751–759, doi:10.1590/s1984-82502016000400020.
11. Pourtalebi Jahromi, L.; Ghazali, M.; Ashrafi, H.; Azadi, A. A Comparison of Models for the Analysis of the Kinetics of Drug Release from PLGA-Based Nanoparticles. *Heliyon* **2020**, *6*, e03451, doi:10.1016/j.heliyon.2020.e03451.